Polarization-selective beam splitter based on a highly efficient simple binary diffraction grating

Danaë Delbeke, Roel Baets, and Peter Muys

A polarization beam splitter (PBS) based on a giant-reflection to zero-order (GIRO) grating is presented. The GIRO grating is a simple binary diffraction grating with parameters chosen such that the excited optical modes in the grating interfere constructively and destructively at the respective interfaces. This interference results in high-zero-order reflection (>99%) with a high polarization-selective extinction ratio (±30 dB). The grating shows a low aspect ratio. The GIRO PBS is theoretically and experimentally shown to be an adequate PBS for use as an optical isolator in combination with a quarter-wave plate in a CO_2-laser system. © 2004 Optical Society of America

OCIS codes: 050.0050, 050.1950, 050.1970, 140.3470, 230.1360, 230.3240.

1. Introduction

Polarization beam splitters (PBSs) are key elements in numerous optical information processing, routing, and imaging systems. The PBS splits an incident beam into two orthogonally polarized light beams. For many years the underlying principle of most PBSs has been based on natural birefringent effects[1] (e.g., Thomson prisms, Nicol prisms, and Wollaston prisms), the refraction effect at multilayer dielectric coatings,[1,2] the absorption effect of a dichroic polarizer,[1] the diffraction effect of grating structures,[3] or a combination of several of these effects.[4,5] Most applications in optical information processing, routing, and imaging systems require that the PBS provide a good extinction ratio, a wide angular bandwidth (a specific behavior valid for a broad angular range), a broad wavelength range for operation with broadband sources, and a small size for effective packaging. These requirements, or a subset, can be met with an appropriate choice of the PBS with an optimized design (see, e.g., Refs. 5–7).

Other applications have other requirements. In particular, the use of PBSs in high-power laser systems (e.g., high-power CO_2 lasers) does not make strong demands on angular bandwidth and wavelength range but requires an extreme extinction ratio and ultrahigh efficiencies. In the manufacturing industry, for applications such as cutting, every loss of photons emitted by multikilowatt lasers affects the efficiency, quality, cutting speed, and cutting characteristics (such as feasible plate thickness) and as such is directly translated into additional costs. Moreover, in this manufacturing industry, optical elements are used in a damaging environment that includes dust and flying splinters. A straightforward fabrication scheme that facilitates the fabrication of the components at low cost is indispensable. The combination of ultrahigh diffraction efficiencies (>99% and <2% for *p* and *s* polarization, respectively) and low-cost implementation demands the use of nonexotic materials with a design that does not challenge technology. In this paper we address a solution to this subset of requirements. We describe the design, fabrication, and characterization of a PBS based on a diffraction grating, namely, a giant-reflectivity to zero-order (GIRO) grating.[8] The GIRO grating combines a high extinction ratio with high efficiency; technological challenges are low owing to a moderate aspect ratio (ratio between grating depth and ridge) and the possibility of using nonexotic materials such as broadly available semiconductor materials (GaAs, InP, etc.). The moderate aspect ratio, in combination with relaxed fabrication tolerances, makes it possible to attain the theoretically required grating parameters and thus the predicted efficiencies (see Section 2 below).[9]

In combination with a quarter-wave plate, a PBS

D. Delbeke (danae.delbeke@intec.ugent.be) and R. Baets are with the Department of Information Technology, Ghent University—Interuniversity Microelectronics Center, St. Pietersnieuwstraat 41, B-9000 Ghent, Belgium. P. Muys is with VDM Laser Optics N.V., Tulpenstraat 2, B-9810 Eke-Nazareth, Belgium.

Received 21 April 2004; accepted 23 July 2004.
0003-6935/04/336157-09$15.00/0

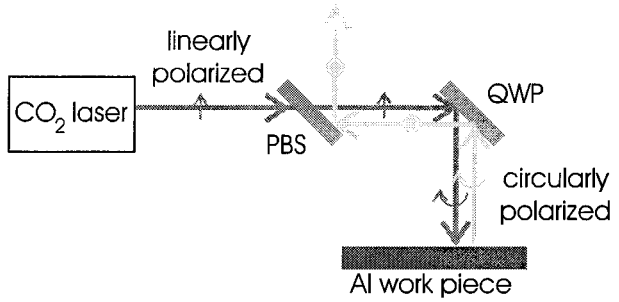

Fig. 1. Schematic of an optical isolator consisting of a PBS and a quarter-wave plate (QWP).

grating placed in the light path of a high-power laser acts as an optical isolator,[10] as is schematically demonstrated in Fig. 1. Linearly polarized light is emitted by the laser. The PBS transmits this polarization with high efficiency. Phase retardation generated by the quarter-wave plate transforms the linear polarization into circularly polarized light. Reflection of the light by the workpiece inverts the sense of circular polarization: It is changed from right to left or vice versa (according to the convention that the rotation sense is defined with respect to the propagation direction). The quarter-wave plate transforms the circular polarization into linear polarization that is orthogonally oriented to the polarization of the originally incoming beam. This polarization is deflected by the PBS grating. The laser is isolated.

It must be stressed that the demands that are addressed (high extinction ratio, ultrahigh efficiencies, and low-cost implementation) are not limited and exclusive to high-power applications. The PBS model proposed in this paper can be applied as such for other applications, e.g., in imaging or routing systems. It is scalable to any desired wavelength and can be extrapolated to a broad range of high-refractive-index material systems, such as ZnSe, GaAs, and InP.

Various kinds of PBS with surface-relief gratings in nonbirefringent substrates have been described theoretically and experimentally in the literature. Polarization selectivity can be obtained by a simple zero-order subwavelength grating. If period Λ of the grating is much smaller than wavelength λ, one can use the effective-medium theory to evaluate the grating diffraction behavior. However, the polarization selectivity (in absolute terms) that can be obtained is minimal.[11] Noponen *et al.* designed a transmissive four-port polarization-sensitive device with a first-order grating that lets light through undiffracted if the light is TM polarized and diffracts the light if TE polarized.[12] A high extinction ratio in combination with high efficiency is theoretically predicted, with a challenging aspect ratio of $\sim$4. The design is limited to low-refractive-index materials ($n \simeq 1.5$). Extrapolation to higher refractive indices requires diffraction angles near 90° for optimizing the polarization properties of the component. The reflection losses tend to increase, and the grating period must be reduced to prevent the emergence of propagating orders inside the material.[13] Lalanne *et al.* achieved this transmissive PBS with $n = 2.3$.[6] They achieved high extinction ratio, but the theoretically predicted efficiency remains below 95%. The aspect ratio is $\sim$4.43.[6] The concept of an optical isolator made from such dielectric diffraction gratings was suggested by Glaser *et al.*[10] The isolator consists of a polarizing first-order grating and a birefringent zero-order grating. The PBS first-order grating is designed for a low-refractive-index material and has an aspect ratio of $\sim$8. Reasonably shallow gratings can be obtained by reflecting PBSs.[3,14] Metallic reflecting PBSs show absorption losses at low operation wavelengths.[15,16] Haidner *et al.*[7] and Kipfer *et al.*[17] measured a surface-relief grating with V grooves in silicon with a metal coating at wavelength $\lambda = 10.6$ μm. The measured diffraction efficiencies were 6% for TE and 92% for TM at normal incidence. Absorption and scattering losses of metallic gratings make those gratings less favorable.

Gori proposed the use of a polarization grating constructed from a series of rotating polarizers.[18] In such gratings the change induced in the polarization is smooth along the transverse direction. Using a periodically (period Λ) spatially variable wave plate, one can use a polarization grating to split the light into two orthogonal polarization states with an angular separation of $\theta = \arcsin(\lambda/\Lambda)$. With the fabrication of this polarization grating based on subwavelength structures, for which the period and the orientation of the subwavelength grooves is space varying, theoretical efficiencies of as much as 100% could be achieved.[19,20] However, these quasi-periodic lamellar subwavelength gratings require a high aspect ratio.[21] Hasman *et al.* experimentally verified the concept of a PBS based on space-variant computer-generated subwavelength structures for CO_2-laser radiation at a wavelength of 10.6 μm. The combination of two Lee-type binary subwavelength structures with an aspect ratio of $\sim$2 results in an efficiency of $\sim$89%.[22]

The GIRO grating used in the PBS discussed in this paper combines a high extinction ratio, high efficiencies, and relaxed technological challenges. The GIRO grating is discussed in more detail in Section 2 below. In Section 3 we describe the use of the GIRO grating as a PBS. Fabrication and experimental results are presented in Section 4.

2. Giant Reflectivity to Zero-Order Grating

A. Modes of the Grating As a Periodic Waveguide

The GIRO grating is in fact a simple binary surface-relief grating but with appropriately chosen grating

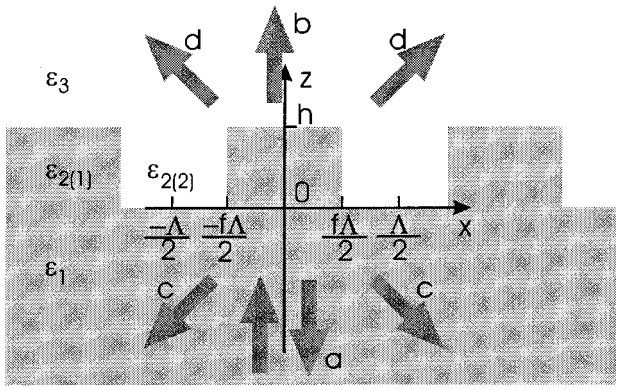

Fig. 2. GIRO grating geometry and parameters.

parameters (Fig. 2). When a monochromatic linearly polarized plane wave is normally incident upon a grating from the high-index side (i.e., from within the dielectric material), the plane wave can couple to the following diffraction orders: the zero order in reflection (wave a), the zero order in transmission (wave b), higher orders in reflection (waves c), and higher orders in transmission (waves d). The grating period is chosen such that

$$\lambda/n_1 < \Lambda < \lambda, \tag{1}$$

i.e., a higher-order grating in the dielectric material with refractive index n_1 and a zero-order grating in air. This choice ensures that only the zero order is present in transmission.

For the binary grating, expressions can be found for the even and odd optical modes that can be excited in the grating layer[23]:

$$\phi_e = \begin{cases} \cos(\gamma_1 x) & 0 \le |x| \le f\Lambda/2 \\ \cos(\gamma_1 f\Lambda/2)\cos\{\gamma_2[|x| - (f\Lambda/2)]\} - (\sigma_2\gamma_1/\sigma_1\gamma_2) & f\Lambda/2 \le |x| \le \Lambda/2\,, \\ \quad \times \sin(\gamma_1 f\Lambda/2)\sin\{\gamma_2[|x| - (f\Lambda/2)]\} & \end{cases} \tag{2}$$

$$\phi_o = \begin{cases} 1/\gamma_1 \sin(\gamma_1 x) & 0 \le |x| \le f\Lambda/2 \\ (1/\gamma_1)\mathrm{sign}(x)(\sin(\gamma_1 f\Lambda/2)\cos\{\gamma_2[|x| - (f\Lambda/2)]\} & f\Lambda/2 \le |x| \le \Lambda/2\,, \\ \quad + (\sigma_2\gamma_1/\sigma_1\gamma_2)\cos(\gamma_1 f\Lambda/2)\sin\{\gamma_2[|x| - (f\Lambda/2)]\}) & \end{cases} \tag{3}$$

with

$$\gamma_j^2 = k_j^2 - \beta^2, \qquad j = 1, 2, \tag{4}$$

$$\sigma_j = \begin{cases} 1 & \text{TE polarization} \\ \epsilon_{2(j)} & \text{TM polarization}\,, \end{cases} \tag{5}$$

where ϕ_e represents the even modes and ϕ_o the odd modes, Λ is the grating period, f is the fill factor of the grating (this is the ratio of the ridge width to the period of the grating), k_1 and k_2 are the wave vectors in the grating region with respective permittivities $\epsilon_{2(1)}$ and $\epsilon_{2(2)}$, and β is the propagation constant in the z direction that is the solution of the dispersion relation of a periodic waveguide[23]:

$$\cos(\gamma_1 f\Lambda)\cos[\gamma_2(1-f)\Lambda] - \frac{1}{2}\left(\frac{\sigma_2\gamma_1}{\sigma_1\gamma_2} + \frac{\sigma_1\gamma_2}{\sigma_2\gamma_1}\right) \times \sin(\gamma_1 f\Lambda)\sin[\gamma_2(1-f)\Lambda] - \cos(k_{x,\mathrm{inc}}\Lambda) = 0, \tag{6}$$

where $k_{x,\mathrm{inc}}$ is the x component of the wave vector of the incident plane wave, which is zero at normal incidence. For simplification of illustration we consider normal incidence and $f = 0.5$. The dispersion relation is then completely defined by grating period Λ/λ and the two material parameters $\epsilon_{2(1)}$ and $\epsilon_{2(2)}$. In Fig. 3 the effective index $n_{\mathrm{eff}} = \beta/k$ is shown for TE and TM polarization for an air–GaAs grating [$n_{\mathrm{GaAs}} = 3.27$ when $\lambda = 10.6\ \mu\mathrm{m}$ (Ref. 24)]. We consider only the $\Lambda/\lambda < 1$ region to obtain a zero-order grating in the air region. In this region (more specifically, at $\Lambda/\lambda < 0.9$), and for the material system considered, there are one odd and two even optical modes. As we consider normal incidence, the grating structure is excited with even excitation, and consequently only the even modes will be excited. Figure 4 illustrates the mode profiles of the zero-order and the second-order modes for TE polarization and TM polarization ($\Lambda/\lambda = 0.64$). Interference effects of these modes will lead to high zero-order TE or TM reflectivities.

B. Design Rules

Based on the mode profiles shown in Fig. 4 and making some rather crude approximations, we can define some simple analytic design rules with which to achieve high zero-order reflectivity. A first approximation concerns the mode profiles in the periodic waveguide (grating). First, the modal profiles of zero-order mode ϕ_0 and second-order mode ϕ_2 are approximated as shown in Fig. 5, which presents the modulus of the electromagnetic field components $|E_y|$ and $|H_y|$. Zero-order mode ϕ_0 is present only in the dielectric material, and second-order mode ϕ_2 is present only in the air gaps between the dielectric ridges. Second, we approximate the reflections at the interfaces as a local phenomenon, i.e., at each point a local reflection coefficient r and a transmission coefficient t are used. These coefficients are given by the Fresnel coefficients for reflection and transmission at planar interfaces for plane-wave incidence. Using these approximations, we approxi-

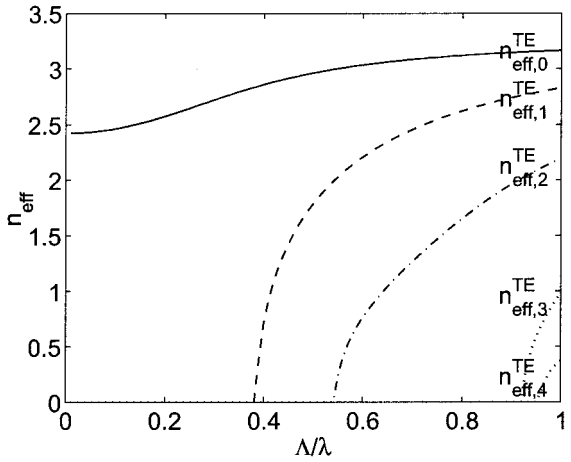

(a)

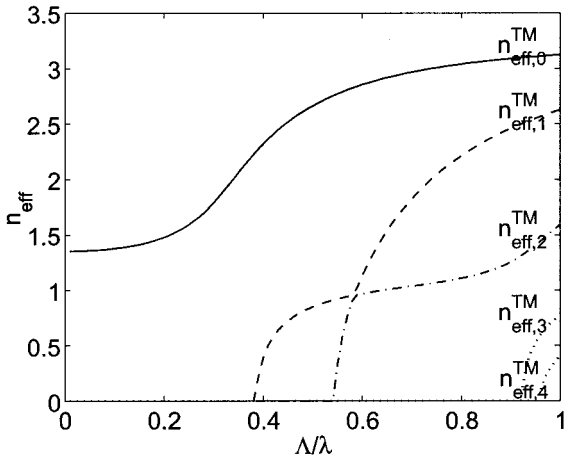

(b)

Fig. 3. (a) Effective index $n_{\mathrm{eff}}^{\mathrm{TE}}$ of the optical modes in the grating structure for TE polarization, (b) effective index $n_{\mathrm{eff}}^{\mathrm{TM}}$ of the optical modes in the grating structure for TM polarization.

mate the reflected field at interface 1 and the transmitted field at interface 2 by ($k = 2\pi/\lambda$):

$$\Phi_1(x) = r[\phi_2(x) + \phi_0(x)\exp(-j2kn_{\mathrm{eff},0}h)], \quad (7a)$$

$$\Phi_2(x) = t[\phi_0(x)\exp(-jkn_{\mathrm{eff},0}h) + \phi_2(x)\exp(-jkn_{\mathrm{eff},2}h)], \quad (7b)$$

which yield for the zero-order power reflection and transmission coefficients, respectively, when they are averaged over one period,

$$R_0 = \left| \int_{-\Lambda/2}^{\Lambda/2} \Phi_1(x)\mathrm{d}x \right|^2, \quad (8a)$$

$$T_0 = \left| \int_{-\Lambda/2}^{\Lambda/2} \Phi_2(x)\mathrm{d}x \right|^2. \quad (8b)$$

With $f = 0.5$ we can say that optical power coupled through the zero order in transmission T_0 is minimal when the average field at interface 2 is zero and that coupling to the zero order in reflection R_0 is maximal when

$$k(n_{\mathrm{eff},0} - n_{\mathrm{eff},2})h = (2m + 1)\pi, \quad (9a)$$

$$2kn_{\mathrm{eff},0}h = 2m'\pi. \quad (9b)$$

In our approximation the zero-order grating mode is concentrated mainly in the material with refractive index $n_{2(1)}$ and is strongly guided. With $f = 0.5$ this leads to a propagation constant β:

$$\begin{aligned}\beta &= \frac{2\pi}{\lambda} n_{\mathrm{eff},0} = (k^2 - k_x{}^2)^{1/2} \\ &= [k^2 - (2\pi/\Lambda)^2]^{1/2} \\ &= (2\pi/\lambda)[n_{2(1)}{}^2 - (\lambda/\Lambda)^2]^{1/2}. \end{aligned} \quad (10)$$

The second-order grating mode is concentrated mainly in the grooves of the grating. Working in the domain for which the slope of $n_{\mathrm{eff},2}$ is the smallest (TM polarization; see below), we can approximate $n_{\mathrm{eff},2}$ by $n_{2(2)} = 1$. This, with $m = 0$ and $m' = 2$ in Eqs. 9(a) and 9(b), respectively, and with Eq. (10), brings us to the following design rules for a grating with $f = 0.5$:

$$\begin{aligned} f &\approx 0.5, \\ h/\lambda &\approx \frac{3/2}{[3n_{2(1)}{}^2 + n_{2(2)}{}^2]^{1/2} - n_2}, \\ \Lambda/\lambda &\approx \frac{2}{[n_{2(1)}{}^2 - n_{2(2)}{}^2]^{1/2}}. \end{aligned} \quad (11)$$

The most important assumption that we made to arrive at these design rules concerns the mode profiles. We assumed that the modes are spatially separated in the grating region, with zero-order mode ϕ_0 present only in the dielectric material and second-order mode ϕ_2 in the air gaps. This limits the application of the design rules to high-refractive-index contrast gratings. Moreover, from Fig. 4 we note that the zero-order TM mode is better confined than the zero-order TE mode in the dielectric material. The TM zero-order mode is thus better estimated by use of Eq. (10). The second-order mode clearly is strongly present in the air regions of the grating (the average field of the second-order mode in the dielectric material is approximately zero) if the effective index of the second-order mode is $n_{\mathrm{eff},2} \approx 1$. Regarding the slope of the effective index (Fig. 3), excitation of the TM second-order mode with specific $n_{\mathrm{eff},2}$ in this region will be less critical than the TE mode. Fine tuning of the grating parameters about the design rules [relations (11)] results in a combination of high reflectivity for TM polarization and low reflectivity for TE.

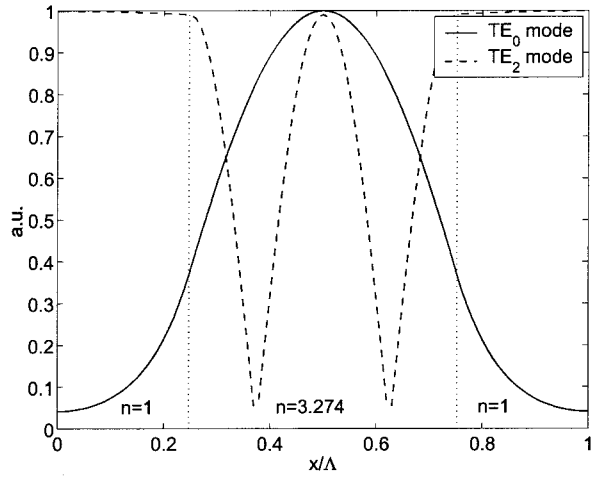

(a)

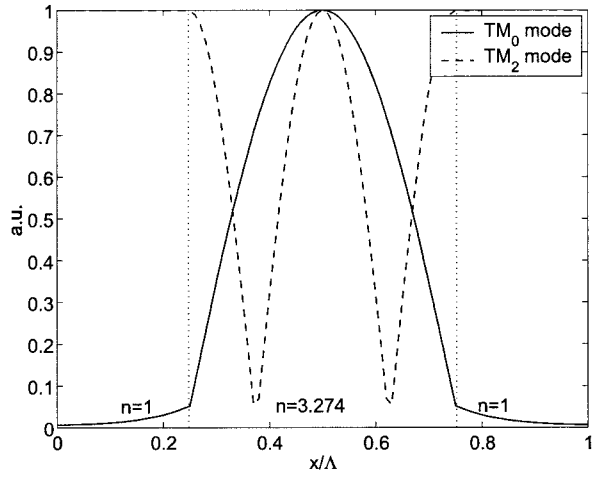

(b)

Fig. 4. Illustration of the mode profiles of the zero-order and the second-order modes for (a) TE polarization ($|E_y|$) and (b) TM polarization ($|H_y|$). $n_{2(1)} = 3.27$, $f = 0.5$, $\Lambda/\lambda = 0.64$.

C. Rigorous Modeling

In view of the rather crude approximations that we used to arrive at the design rules of relations (11) for high-zero-order TM reflectivity and to show the necessity for fine tuning to arrive at a high extinction ratio, a design based on the design rules is compared with a design based on rigorous calculations. To this end, the rigorous coupled-wave analysis (RCWA) for gratings that was proposed by Moharam *et al.*[25,26] and reformulated by Li[27] and Lalanne[28] to improve TM convergence has been implemented. Figure 6 shows the numerical calculations of the zero-order TE and TM reflectivity for normal incidence. TM reflectivity remains high for a Λ/λ range that corresponds to the low-slope region of $n_{\mathrm{eff},2}$, whereas TE reflectivity varies within that range. Table 1 compares the start values obtained by the design rules

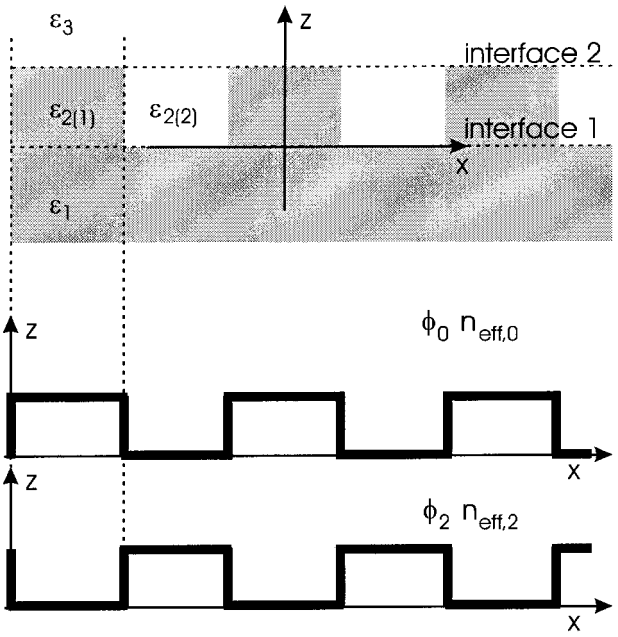

Fig. 5. GIRO grating (top) and approximation for the optical modes in the grating layer.

with the optimized values calculated with the RCWA. We can conclude that the optimum parameter set for the GIRO gratings is quite well predicted by the design rules. The TM reflectivity of the fine-tuned design is as high as 99.3% in combination with an extinction ratio of 32.2 dB. The aspect ratio of the grating is only 0.98.

D. Sensitivity to Parameter Changes

Variations of period Λ and thickness h of the GIRO grating affect the diffraction efficiency and the extinction ratio as shown in Fig. 6. It is clear that the allowable range of variation about the optimal value for both Λ and h resides in the technologically attainable accuracy, especially for $\lambda = 10.6$ μm.

The influence of the angle of incidence on the behavior of the GIRO grating is presented in Fig. 7. Incidence angle θ is defined in the plane spanned by the Bragg vector and the surface normal; incidence angle α, in the plane normal to the latter plane. Both angles are defined in the surrounding air medium. With a variation of ~10 deg for α and a couple of degrees for θ, the design is adequate to be used in realistic alignment systems for high-power laser optics.

Figure 8 shows the diffraction efficiency of the GIRO grating on a function of a varying fill factor f and of wavelength λ. It is clear that, during the fabrication of the grating, good control of fill factor f is needed, as that factor is the most critical parameter of the GIRO grating. The low aspect ratio of the GIRO grating eases the technological challenges required for obtaining fill factor f in the accepted range.

3. Polarization Beam Splitter

The GIRO grating shows high zero-order TM reflectivity only when light is incident from the high-

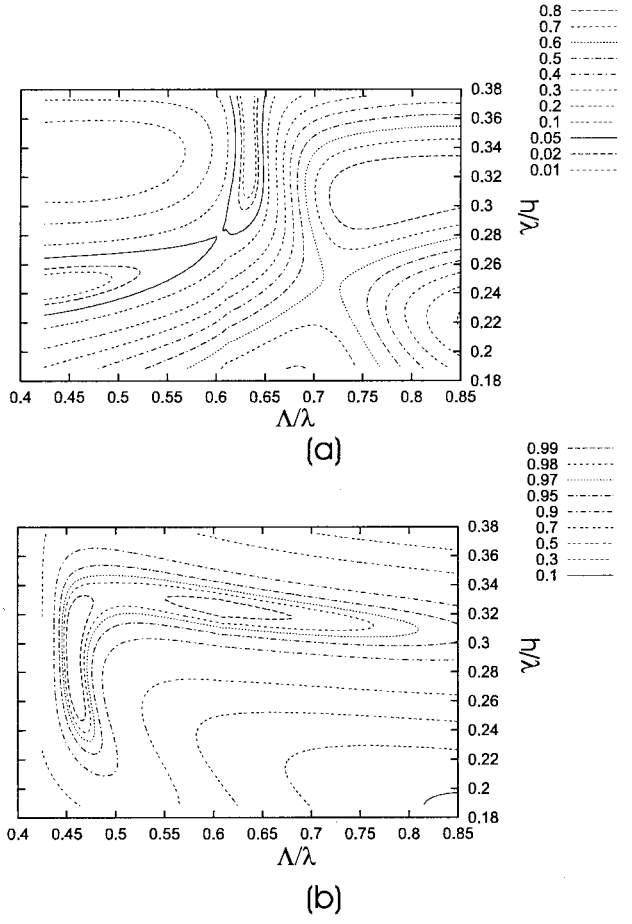

Fig. 6. Simulations of zero-order (a) TE reflectivity and (b) TM reflectivity over a large h/λ and Λ/λ range (normal incidence, $f = 0.5$, $n = 3.27$).

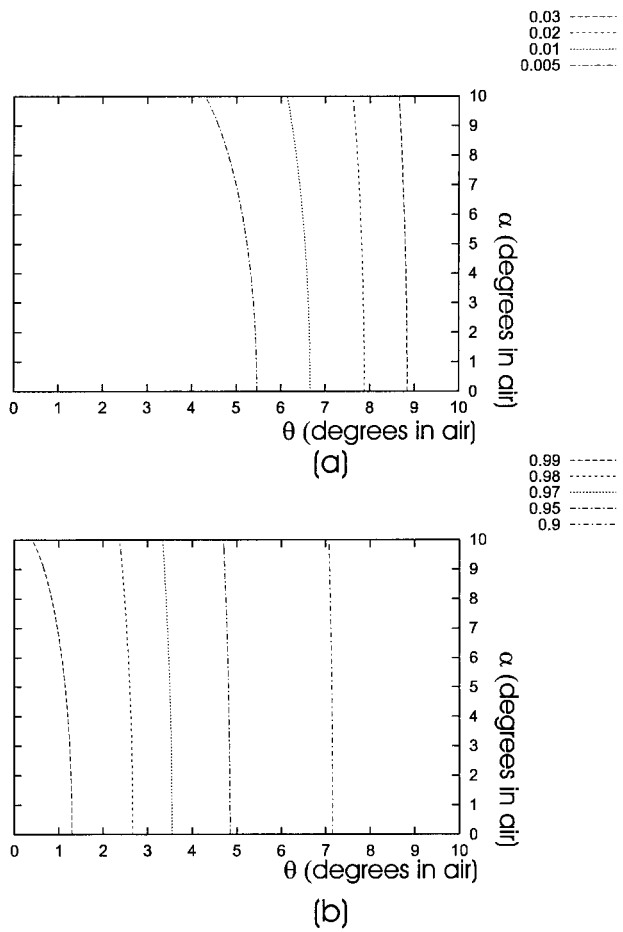

Fig. 7. RCWA simulations of diffraction efficiencies (a) R_0^{TE} and (b) R_0^{TM} as functions of incidence angle. $f = 0.5$, $h/\lambda = 0.323$, $\Lambda/\lambda = 0.634$, $n = 3.27$.

refractive-index material. This implies that the GIRO grating cannot as such be used as a PBS but that a configuration is needed as sketched in Figs. 9(a) and 2(b). An antireflection coating prevents reflections at the high-contrast index interface [air ($n = 1$)/GaAs ($n = 3.27$)]. This prevents the creation of a Fabry–Perot resonator and thus guarantees high TM reflectivity, independently of the thickness of the wafer. TE-polarized light incident upon the GIRO grating is partially transmitted ($T_0^{TE} \approx 0.7$) in the first diffraction order and partially reflected ($R_{\pm 1}^{TE} \approx 0.1$) in the second diffraction order. The higher diffraction orders are totally internally reflected at the high-contrast index interface, irrespective of the presence of an antireflection coating. This would disturb the PBS if the wafer thickness were not chosen so thick as to prevent backreflection on the grating. Moreover, inclined facets are polished on the wafer sides toward which the light is diffracted [inclination angle, $\beta = a \sin(\lambda/n/\Lambda)$]. TE-polarized light, reflected by the GIRO grating into the first diffraction orders, is guided in the substrate toward these inclined facets. Normal incidence on these facets, provided by an antireflection coating, permits maximal escape of the TE light from the substrate.

Table 1. Comparison of GIRO Grating Designs Based on the Design Rules and on Calculations by RCWA[a]

Method of Calculation	Parameter			
	h/λ	Λ/λ	R_0^{TM}	R_0^{TE}
Design rules	0.315	0.6412	0.986	0.017
RCWA	0.323	0.634	0.993	0.0006

[a]Refractive index, $n_{2(1)} = 3.27$; $f = 0.5$.

The GIRO grating is a reflective element that, in normal conditions, works under normal incidence. As can be seen from Fig. 7, high efficiency in combination with a high extinction ratio can still be achieved when the angle of incidence is chosen to be $\theta = 0°$ or $\alpha = 5°$. The configuration of the PBS is then as sketched in Fig. 9(c). Similar Z configurations (e.g., reflective beam expanders) are commercially available already. They have the advantage of not altering the light-path direction.

4. Fabrication and Experimental Results

A GIRO grating was fabricated in undoped GaAs to serve as a PBS for a CO_2 laser. Photolithographic

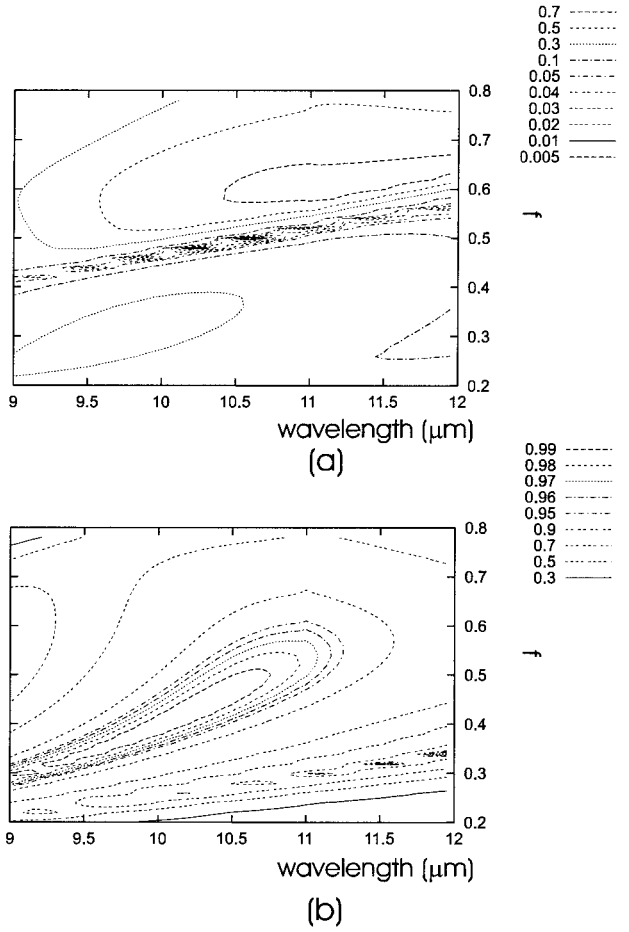

Fig. 8. RCWA simulations of the diffraction efficiencies (a) R_0^{TE} and (b) R_0^{TM} as functions of fill factor f and wavelength λ. $\theta = \alpha = 0$, $h/\lambda = 0.323$, $\Lambda/\lambda = 0.634$, $n = 3.27$.

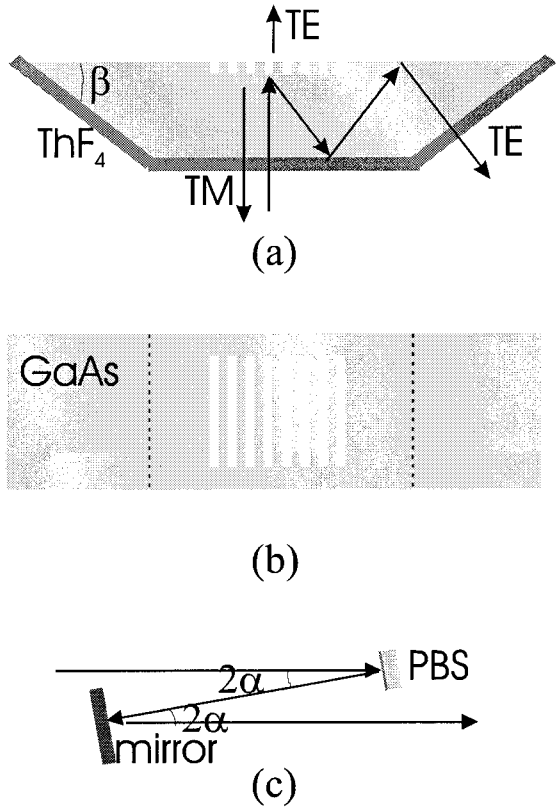

Fig. 9. PBS based on a GIRO grating.

illumination ($\lambda = 310$ nm) of a chromium mask was used to define the grating in photoresist (AZ5214) spun onto the GaAs wafer. After development of the resist in a potassium hydroxide dilute solution and a postbake, the resist pattern was transferred into a semiconductor by use of an inductive coupled plasma reactive-ion etching system. The system uses a $SiCl_4$–Ar gas mixture at a pressure of 16 m Torr, a rf power of 150 W and an inductive coupled plasma power of 50 W. This process is optimized to produce steep sidewalls (binary gratings with a crenellated shape) and etches at a rate of 300 nm/min. The photoresist on top of the GaAs grating is removed by acetone. A scanning-electron microscope picture of a grating etched by this process into an undoped GaAs wafer of thickness 500 μm is presented in Fig. 10(a). Excellent control of the steepness of sidewalls, fill factor f, and etch depth (±25 nm) is achieved. This process was optimized and used for definition of the grating in a wafer with a thickness of ±3 mm. However, Fig. 10(b) shows a decreased smoothness of the sidewalls. The reason for this inaccuracy when thick wafers are used is not clear. Temperature, gas flow, and material quality are some possible factors. Figure 10(c) shows a picture of the PBS.

The PBS was illuminated with a CO_2 laser at 10.6 μm with a beam waist of 5 mm. The incident intensity was ~40 W/cm^2, which did not heat the grating in a noticeable way. The reflected, transmitted, and incident power was measured with a large area detector for both TE and TM linearly polarized light. Table 2 compares experimental results with theoretical ones. An optimal GIRO grating (Table 1) results theoretically in a zero-order TM reflectivity of 99.2% and a zero-order TE reflectivity of 0.13% for incidence angles $\theta = 0°$ and $\alpha = 5°$. Experimentally, we measured a zero-order TM reflectivity of 94.1% and a zero-order TE reflectivity of 1.3%. Deviation of the achieved grating from the ideal binary grating [as shown in Fig. 10(b)] resulted in a somewhat lower efficiency and extinction ratio than those of the optimal theoretical GIRO grating. The experimental results correspond better to theoretical results when the fabricated structure, as shown in Fig. 10(b), i.e., a grating with a nonoptimal binary crenellated shape is simulated (Table 2). We can conclude that when the technical process for etching gratings in thick GaAs wafers is as good as the process for etching gratings in standard 500-μm wafers (which is a matter of etch parameter optimization), high efficiency (~99%) in combination with a high extinction ratio (~30 dB) can be expected.

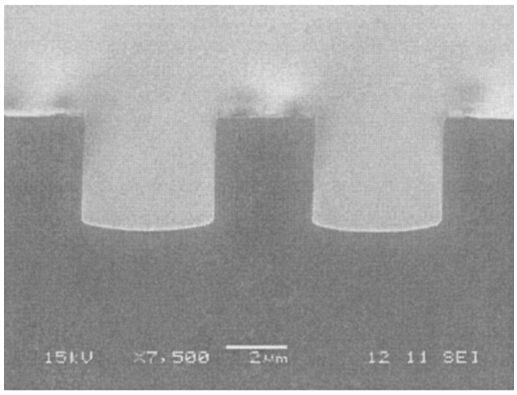

(a)

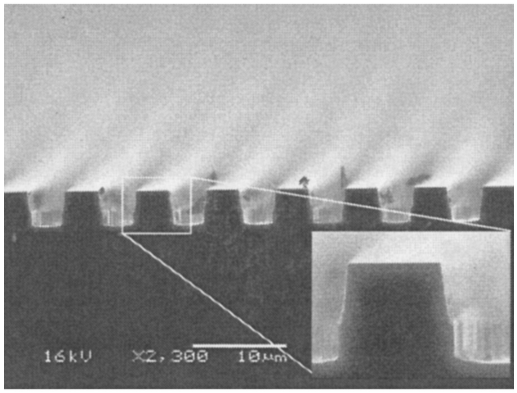

(b)

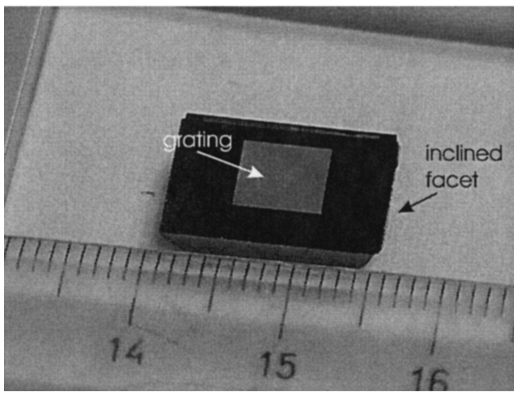

(c)

Fig. 10. Scanning-electron microscope picture of a GIRO grating in undoped GaAs with (a) a wafer thickness of 500 μm and (b) a wafer thickness of 3 mm. (c) PBS.

Table 2. PBS Based on a GIRO Grating: Comparison of Theoretical and Experimental Results

Simulation versus Measurement	R_0^{TM}	R_0^{TE}
Simulation of optimal GIRO	0.992	0.0013
Measured PBS	0.941	0.013
Simulation of achieved GIRO	0.94	0.06

5. Conclusions

A highly efficient PBS with a high extinction ratio has been described. The PBS, which can be used in combination with a quarter-wave plate as an optical isolator, is based on the use of a GIRO grating. The GIRO grating is a simple diffractive binary grating that shows extremely high diffraction efficiencies in combination with a high extinction ratio. Its parameters were chosen on the basis of design rules that guarantee destructive interference of the optical modes in the grating at one interface and constructive interference at the other interface. The optical modes need good confinement in the grating structure, which occurs only for TM polarization in high-refractive-index gratings. Fine tuning of the grating resulted in a theoretical TM zero-order reflectivity of 99.2% and a TE zero-order reflectivity of 0.13%. The design will be used for high power CO_2 lasers (wavelength, 10.6 μm); the material is GaAs ($n = 3.27$) and the incidence angle is 5°. With period $\Lambda/\lambda = 0.634$ and depth $h/\lambda = 0.323$ the aspect ratio was only 0.98, simplifying the technology remarkably. The PBS was fabricated by a standard photolithographic process that is used in commercial fabrication. Although the process is standard and well controlled when standard GaAs wafers (with a thickness of 500 μm) are used, the GIRO grating was not perfectly binary when thick GaAs wafers (with a thickness of 3 mm) were used. The process parameters need to be adapted. Notwithstanding these solvable technological shortcomings, experimental polarization splitting has been observed with high efficiency ($R_0^{TM} = 94.1\%$) and a high extinction ratio (18.6 dB) has been observed.

High efficiency, a high extinction ratio, a straightforward processing scheme, and a design with reasonable tolerances make the GIRO PBS an excellent candidate to be used in high-power laser applications. Nevertheless, the GIRO PBS can be used straightforwardly in other applications such as imaging and routing.

D. Delbeke thanks the Institute for the Promotion of Innovation by Science and Technology in Flanders for financial support. The authors are grateful to Bart Dhoedt and Stefan Goeman for exploring research on the GIRO grating and to Steven Verstuyft and Liesbet Van Landschoot for technical support.

References

1. F. A. Jenkins and H. E. White, *Fundamentals of Optics* (McGraw-Hill, New York, 1957), Chap. 24.
2. L. Li and J. A. Dobrowolsky, "High-performance thin-film polarizing beam splitter operating at angles greater than the critical angle," Appl. Opt. **39,** 2754–2771 (2000).
3. J.-L. Roumiguieres, "The rectangular-groove grating used as an infrared polarizer," Opt. Commun. **19,** 76–78 (1976).
4. R. Liu, B.-Z. Dong, G.-Z. Yang, and B.-Y. Gu, "Optimal design of polarizing beam splitters with a birefringent substrate," J. Opt. Soc. Am. A **14,** 49–53 (1997).
5. R.-C. Tyan, A. A. Salvekar, H.-P. Chou, C.-C. Cheng, A. Scherer, P.-C. Sun, F. Xu, and Y. Fainman, "Design, fabrication, and characterization of a form-birefringent multilayer polarizing beam splitter," J. Opt. Soc. Am. A **14,** 1627–1637 (1997).
6. P. Lalanne, J. Hazart, P. Chavel, E. Cambril, and H. Launois,

"A transmission polarizing beam splitter," J. Opt. A **1,** 215–219 (1999).
7. H. Haidner, P. Kipfer, J. T. Sheridan, J. Schwider, N. Streibl, J. Lindolf, M. Collischon, A. Lang, and J. Hutfless, "Polarizing reflection grating beamsplitter for the 10.6-μm wavelength," Opt. Eng. **32,** 1860–1865 (1993).
8. R. Baets, B. Demeulenaere, B. Dhoedt, and S. Goeman, "Optical system with a dielectric subwavelength structure having high reflectivity and polarization selectivity," U.S. patent 6,191,890 (20 February 2001).
9. S. Goeman, S. Boons, B. Dhoedt, K. Vandeputte, K. Caekebeke, P. Van Daele, and R. Baets, "First demonstration of highly reflective and highly polarization selective diffraction gratings (GIRO-gratings) for long-wavelength VCSEL's," IEEE Photon. Technol. Lett. **10,** 1205–1207 (1998).
10. T. Glaser, S. Schröter, H. Bartelt, H.-J. Fuchs, and E.-B. Kley, "Diffractive optical isolator made of high-efficiency dielectric gratings only," Appl. Opt. **41,** 3558–3566 (2002).
11. S. Chou and W. Deng, "Subwavelength amorphous silicon transmission gratings and applications in polarizers and waveplates," Appl. Phys. Lett. **67,** 742–744 (1995).
12. E. Noponen, A. Vasara, J. Turunen, J. M. Miller, and M. R. Taghizadeh, "Synthetic diffractive optics in the resonance domain," J. Opt. Soc. Am. A **9,** 1206–1213 (1992).
13. M. Kuittinen, J. Turunen, and P. Vahimaa, "Subwavelength-structured elements," in *Diffractive Optics for Industrial and Commercial Applications*, J. Turunen and F. Wyrowski, eds. (Akademie-Verlag, Berlin, 1997), pp. 303–323.
14. K. Knop, "Reflection grating polarizer for the infrared," Opt. Commun. **26,** 281–283 (1978).
15. C. R. A. Lima, L. L. Soares, L. Cescato, and A. L. Gobbi, "Reflecting polarizing beam splitter," Opt. Lett. **22,** 203–205 (1997).
16. L. L. Soares and L. Cescato, "Metallized photoresist grating as a polarizing beam splitter," Appl. Opt. **40,** 5906–5910 (2001).
17. P. Kipfer, M. Collischon, H. Haidner, J. T. Sheridan, J. Schwider, N. Streibl, and J. Lindolf, "Infrared optical components based on a microrelief structure," Opt. Eng. **33,** 79–84 (1994).
18. F. Gori, "Measuring Stokes parameters by means of a polarization grating," Opt. Lett. **24,** 584–586 (1999).
19. J. Tervo and J. Turunen, "Paraxial-domain diffractive elements with 100% efficiency based on polarization gratings," Opt. Lett. **25,** 785–786 (2000).
20. J. A. Davis, J. Adachi, C. R. Fernandez-Pousa, and I. Moreno, "Polarization beam splitter using polarization diffraction grating," Opt. Lett. **26,** 587–589 (2001).
21. L. Pajewski, R. Borghi, G. Schettini, F. Frezza, and M. Santarsiero, "Design of a binary grating with subwavelength features that acts as a polarizing beam splitter," Appl. Opt. **40,** 5898–5905 (2001).
22. E. Hasman, Z. Bomzon, A. Niv, G. Biener, and V. Kleiner, "Polarization beam-splitters and optical switches based on space-variant computer-generated subwavelength quasi-periodic structures," Opt. Commun. **209,** 45–54 (2002).
23. L. Li, "A modal analysis of lamellar diffraction gratings in conical mountings," J. Mod. Opt. **40,** 553–573 (1993).
24. M. R. Brozel and G. E. Stillman, eds., *Properties of Gallium Arsenide* (INSPEC, London, 1996).
25. M. G. Moharam, E. B. Grann, D. A. Pommet, and T. K. Gaylord, "Formulation of stable and efficient implementation of the rigorous coupled-wave analysis of binary gratings," J. Opt. Soc. Am. A **12,** 1068–1076 (1995).
26. M. G. Moharam, D. A. Pommet, E. B. Grann, and T. K. Gaylord, "Stable implementation of the rigorous coupled-wave analysis for surface-relief gratings: enhanced transmittance matrix approach," J. Opt. Soc. Am. A **12,** 1077–1086 (1995).
27. L.-F. Li, "Use of Fourier series in the analysis of discontinuous periodic structures," J. Opt. Soc. Am. A **13,** 1870–1876 (1996).
28. P. Lalanne, "Effective properties and band structures of lamellar subwavelength crystals: plane-wave method revisited," Phys. Rev. B **58,** 9801–9807 (1998).